Small-scale sedimentary structures and permeability in a cross-bedded aquifer

Marijke Huysmans[(1)] (corresponding author), Luk Peeters[(1)], Gert Moermans[(1)] and Alain Dassargues[(1,2)]

[(1)] Katholieke Universiteit Leuven
Applied Geology and Mineralogy
Celestijnenlaan 200 E
3001 Heverlee
Belgium
Tel: +32 16 32 64 49
Fax: +32 16 32 29 80

[(2)] Université de Liège
Hydrogeology and Environmental Geology
Department of Architecture, Geology, Environment, and Civil Engineering (ArGEnCo)
B.52/3 Sart-Tilman
4000 Liège
Belgium

E-mail: marijke.huysmans@geo.kuleuven.be

Abstract

This paper investigates the relations between small-scale sedimentary structures and permeability in the Brussels Sands formation, an early Middle-Eocene shallow marine sand deposit in Central Belgium. A field campaign is carried out consisting of field observations of the sedimentary structures and *in situ* measurements of air permeability. The sedimentary structures are sketched, photographed and measured. Additionaly, a total of 2750 cm-scale air permeability measurements are carried out *in situ*. Comparison between the sedimentary structures and permeability shows that clay-rich sedimentary features such as bottomsets and distinct mud drapes exhibit a different permeability distribution than the rest of the cross-bedded sands. Another interesting result is that anisotropy in the cross-bedded sands is dominated by the foreset lamination orientation. The results thus show that the sedimentary heterogeneity results in a clear permeability heterogeneity.

1. Introduction

Small-scale permeability heterogeneity related to sedimentary structures is usually not taken into account in groundwater and solute transport modelling. In petroleum reservoir modelling however, several authors acknowledge that fine-scale sedimentary heterogeneity plays an important role in oil recovery and that incorporating this small-scale sedimentary heterogeneity is required for reliable prediction of oil production (e.g., Mikes, 2006; Morton et al., 2002; Willis and White, 2000). Since this small-scale sedimentary heterogeneity plays such an important role in reservoir modelling, it is likely that this may also be important in

hydrogeology, especially in transport modelling. Therefore, this paper investigates the importance of small-scale sedimentary heterogeneity in hydrogeological studies.

The measurement campaign described in this paper is part of a project about modeling groundwater flow and transport in heterogeneous environments with complex geological structures. In this project, the effect of geological structures, mainly sedimentary features, on permeability heterogeneity and consequently on groundwater flow and transport is studied. This paper describes the first part of this project, which is an extensive field campaign to unravel the relation between sedimentary structures and permeability in a sandy aquifer.

The aquifer under study is the Brussels Sands formation, which is a major source of groundwater in Belgium. Approximately 29,000,000 m^3 of groundwater per year is pumped from this aquifer. The Brussels Sands display a complex geological heterogeneity and anisotropy which has resulted in the past in problems with pumping test interpretation, groundwater models and prediction of pollutant transport

To investigate the relationship between sedimentary structures and permeability at a cm-scale to m-scale, pumping tests and slug tests are not useful since they provide permeability information on a much larger scale. Therefore, an *in situ* air permeameter is used to determine permeability at a small-scale. Air permeameters have been used in a wide variety of laboratory and field applications where localized small-scale measurements are needed to characterize the spatial distribution of permeability. Air permeameter measurements have the advantage to be cheap, rapid, nondestructive and readily repeatable and can provide a high resolution, almost continuous profile of permeability distribution. *In situ* permeameters can reveal several orders of magnitude of permeability contrast missed by conventional core plug measurements (Goggin et al., 1988; Halvorsen and Hurst, 1990). Air permeameter measurements are particularly suitable for poorly consolidated and laminated materials, both of which may present problems for permeability characterization using core plugs (Hurst and Goggin, 1995). Potential disadvantages of air permeability measurements are the sensitivity of probe permeameter response to partial or full saturation and sample surface effects such as irregularities and weathering, the limited knowledge about the geometry of flow paths in probe permeameter experiments and the requirement that outcrops should be completely dry or their relative permeability to gas and water should be known to allow satisfactory interpretation of the data.

2. Materials and Method

2.1 Geological setting

All observations and measurements are made in a Brussels Sands quarry in Bierbeek near Leuven in Belgium (Fig. 1). The Brussels Sands formation is an early Middle-Eocene shallow marine sand deposit in Central Belgium. The sands consist of unconsolidated quartz sands with variable percentages of feldspars, silex, glauconite, carbonates and heavy minerals. The Brussels Sands are a tidal sandbar deposit, deposited at the beginning of an important transgression at the southern border of the Eocene North Sea. The Brussels Sands base has an erosive character which is thought to be related to a strong SSW-NNE tidal current that produced longitudinal troughs. Transverse sandbars that migrated to the north filled these rapidly shifting channels. The tidal regime was strongly asymmetric and ebb-dominated with a NNE oriented main tidal flow. In a first depositional stage, large amounts of clastic sands mixed with coarse glauconite are deposited as thick cross-beds filling tide-parallel channels of

a few kilometres wide and tens of meters deep. In a later depositional stage, the supply of glauconite ended and finer, carbonate-rich sands were deposited (Houthuys, 1990).

The depositional environment of the Brussels Sands is studied in detail by Houthuys (1990) based on field studies and descriptions of approximately 90 outcrops and hundreds of boreholes. His work describes several features and sedimentary structures typical for tidal deposits such as important grain size variations, cross-bedding, bottomsets, foresets, mud drapes and unidirectional reactivation surfaces (Fig. 2). Cross-bedding is defined as the disposition of laminations tranverse or obliquely inclined to the main stratification of the bedding planes (Whittow, 2000). Cross-bedding in the Brussels Sands is caused by sediment deposition at the leeside of migrating sandbars. Bottomset beds are formed in front of the leeside of migrating sandbars and consist of finer grained sediment. Foreset deposits consist of laminae that formed by grains avalanching down the leeside of sandbars. The inclined foreset laminae are preserved in sequence in the sandbodies and are a record of successively earlier positions of the leesides. The grains are sorted during avalanching, resulting in coarse and fine grained laminae (Hartkamp et al., 1993). Mud drapes are thin layers of mud covering the complete seafloor during turning of the tide (Houthuys, 1990). Reactivation surfaces are produced when the lee side of a sandbar is partially eroded.

2.2 Field observations of sedimentary structures

The sedimentary structures of the cross-bedded facies of the Brussels Sands are described and interpreted in the Brussels Sands quarry in Bierbeek near Leuven (Belgium). The outcrop is mapped in detail with regard to sedimentary structures and lithologies. Geological sketches and pictures from all faces of the quarry are made. Clay-rich bottomsets and distinct mud drapes in the foresets are identified. Measurements are made of the set thicknesses, master bedding dipping angles, bottomset thicknesses, foreset lamination thicknesses and lamination dipping angles. These measurements are compared with data from Houthuys (1990) and analysed statistically.

2.3 In situ permeability measurements

Permeability of the Brussels Sands is measured on all faces of the same Brussels Sands quarry in Bierbeek near Leuven (Belgium) using a portable *in situ* air permeameter. A device for obtaining small-scale air permeability measurements was first described by Dykstra and Parsons (1950). Later, Eijpe and Weber (1971) constructed a minipermeameter for measuring the permeability of rock and unconsolidated sands. A probe permeameter is basically an annulus through which gas (nitrogen or air) can be released into porous media. Leakage between the annulus and the porous media is avoided by placing a ring of compressible, impermeable material at the probe tip. Gas flow rate and gas pressure are monitored and can be transformed into gas permeability by empirically derived relationships or by use of an analytical equation, such as the modified form of Darcy's law including a geometrical factor depending on tip seal size proposed by Goggin et al. (1988):

$$k = \frac{2\mu P_1 Q_1}{\left(P_1^2 - P_2^2\right) G_0^a} \qquad (1)$$

where k is permeability, μ is the gas viscosity at atmospheric pressure, P_1 is injection pressure, P_2 is outflow pressure, Q_1 is the volumetric rate at injection pressure P_1, G_0 is a dimensionless geometric factor and a is the radius of the seal area. For certain ranges of permeability,

equation (1) should be corrected to account for gas slippage and high velocity gas flow effects (Goggin et al., 1988). The depth of investigation of a minipermeameter is approximately four times the internal radius of the tip seal according to Goggin *et al.* (1988). In an isotropic porous medium, the measurement volume would correspond to a hemispherical shaped volume of rock with radius of approximately four times the internal radius of the tip seal. Jensen et al. (1994) found that probe permeameter measurements are even more localized with a depth of investigation of the order of only two probe inner radii.

In this study, air permeability is measured using the TinyPerm II distributed by New England Research (NER). Permeability measurements are taken by pressing the device against the quarry face and depressing the plunger to withdraw air from the porous medium. Leakage between the annulus and the rock is avoided by a compressible, impermeable rubber tip. The inner tip diameter is 9 mm and the outer tip diameter is 24 mm. According to the equations of Goggin et al. (1988), this means that the depth of investigation of TinyPerm is approximately 18 mm. The measurement volume is in this case a hemispherical shaped volume with a radius of approximately 18 mm. A micro-controller unit simultaneously monitors the syringe volume and the transient vacuum pulse created at the sample surface. Using signal processing algorithms the micro-controller computes the response function of the sample/instrument system. This response function is related to the air permeability of the sample, which can be determined by an equipment specific calibration curve provided by NER. Measurements of high permeability samples take a few seconds, measurements of less permeable samples take up to a few minutes.

To prevent loose sand debris being sucked into the device, a metal screen is fitted in the rubber tip for this study. After installation of this filter, the TinyPerm II is recalibrated since the filter can impede air flow. Rock samples with different permeabilities are measured with and without the filter to obtain a calibration curve for the device equipped with a filter. The sample set for recalibration consists of seven sandstone samples, a limestone sample and a chalk sample. All rock samples have a smooth to slightly irregular surface. The permeabilities of the calibration set range from 1 to 10,000 mD which is within the measurement range of the TinyPerm II air permeameter. Each sample was measured six times: three times without filter and three times with filter. As expected, permeability values measured with the filter were slightly smaller than permeability values measured without the filter. Permeability values with filter were on average 89% of permeability values measured without filter. To correct for this effect, the TinyPerm II response function of the measurements with filter was plotted against the permeability values obtained without a filter using the calibration curve provided by NER. This yields a calibration curve for the device after installation of the filter.

Measurements in the Bierbeek quarry are taken on several rectangular regular grids on different walls in dry conditions. All irregularities and weathered or loose material is removed prior to constructing the grids. The measurement spacing is adjusted to the lamina thickness so that the vertical and horizontal spacing is between 2 and 5 cm. Total grid dimensions are between 40 cm and 1 m. A total of approximately 2750 air permeability measurements are made on outcrops with different orientations in the Bierbeek quarry. The measured permeability values are compared with Brussels Sands permeability values from literature. The measured permeability values are also compared with the sedimentary facies and structures observed at the same location.

All 2750 permeability data are also analysed statistically and geostatistically. Permeability variograms are calculated and modelled using Stanford Geostatistical Earth Modeling

Software (S-GEMS). The variogram is the most familiar geostatistical estimator and is defined as half of the average squared difference between variable values separated by a lag vector **h**:

$$\gamma(\mathbf{h}) = \frac{1}{2N(\mathbf{h})} \sum_{i=1}^{N(\mathbf{h})} (x_i - x_i')^2$$

where $N(\mathbf{h})$ is the number of pairs and x_i and x_i' are a data pair separated by **h**. The semivariogram can be understood as the sample variance described as a function of spatial separation. Low semivariogram values indicate a high degree of correlation between variable values separated by the lag vector, while high semivariogram values indicate a low degree of correlation. Variograms are usually modeled with a variogram model. The model used in this study is the sum of a nugget model and a spherical model:

$$\gamma(h) = \begin{cases} 0 & if\ h = 0 \\ C_0 + C(1.5\frac{h}{a} - 0.5\left(\frac{h}{a}\right)^3) & otherwise \\ C_0 + C & if\ h > a \end{cases}$$

where C_0 is the nugget effect, C is the sill and a is the range (Fig. 3).

3. Results and discussion

3.1 Sedimentary structures

The sedimentary structures observed in the Bierbeek quarry correspond to the descriptions of Houthuys (1990). The Brussels Sands in this quarry consist of parallel sub-horizontal tabular sets dipping approximately 1° to the NNE (Fig. 4). The set thickness is usually approximately 1 m and may be up to 2.5 m. Individual sets can be followed over distances as large as the quarry dimensions in the paleoflow direction. In a perpendicular section, individual sets dipping up to 5° occur in wedge-shaped groups alternately deposited on the east and west side of a channel. These individual sets can be followed over tens of meters in a section perpendicular to the paleoflow direction (Fig. 4). Most beds include a thick bottomset consisting of finer grained material at the base. These bottomsets are usually about 10 cm thick, and may exceptionally be maximum 50 cm thick. The bottomsets sometimes show a lateral thickness variation. The foresets have a lamination thickness of 0.5 to 3 cm and dip approximately 25-30° to the NNE. Thin mud drapes consisting of fine silt and clay occur in the foreset laminae resulting in grain size contrasts. The mud drapes are best developed near the toesets and wedge out in the upper part of the foresets. Lateral variations in the amount of mud drapes occur due to neap/spring cycles. Mud drapes are not always laterally continuous perpendicular to the paleoflow direction.

A visual distinction between sand-rich and clay-rich zones is made in situ. The sand-rich zones consist of cross-bedded sands while the clay-rich zones consist of clay-rich bottomsets and distinct mud drapes inside the cross-beds. Figure 5 shows an interpreted photomosaic of one of the quarry walls, corrected for perspective distortion. On this photograph, the clay-rich bottomsets and distinct mud drapes in the foresets that are visually identified *in situ* are marked.

Thickness and dip measurements of several sedimentary features are made in the quarry and analysed statistically. Histograms of bottomset thicknesses, set thicknesses and lamination dipping angles measured during this measurement campaign combined with the data from

Houthuys (1990) are shown in Figure 6. Bottomset thickness varies between 0 and 38 cm in the Bierbeek area and is 11 cm on average. The average set thickness is 79 cm. Foreset lamination dip is between 10 and 33° with an average value of 25°.

3.2 Permeability

Measured air permeability using the TinyPerm air permeameter in the Bierbeek quarry lies between 11,000 mDarcy and 125,000 mDarcy. These values are compared to values derived from well tests carried out at different locations in the Brussels Sands. Hydraulic conductivity from pumping tests and piezometer tests is between 4.6×10^{-6} and 3.4×10^{-4} m/s (Bronders, 1989), which corresponds to intrinsic permeability values between 675 and 40,000 mDarcy. Permeability values measured using the in situ air permeameter are thus characterized by a higher average value and a higher variability than the values derived from well tests. The higher average value is logical since the Bierbeek quarry is located in one of the coarsest and most permeable facies of the Brussels Sands (Houthuys, 1990). The higher variability of the air permeability measurements is related to the measurement scale. Since the well tests have a much larger measurement volume than the air permeability measurements, permeabilities measured by well tests are averages of permeabilities in this large measurement volume and show less variability than smaller scale measurements.

3.3 Relation between sedimentary structures and permeability

This paragraph discusses the relations between measured air permeability and the observed sedimentary structures. First, results of individual measurements grids at different locations are discussed separately. Secondly, all 2750 measurements are compiled and analyzed statistically and geostatistically.

Figures 7 and 8 show the results of observations of sedimentary structures and measurements of permeability on a 1 m by 1 m regular grid on a N40°E oriented face. On this grid, 400 air permeability measurements are made at a spacing of 5 cm. Different lithologies are present in this grid: cross-bedded sands, some clay-rich bottomsets and distinct mud drapes and cemented concretions. At some locations, measuring permeability was impossible due to irregular shaped concretions, surface conditions or vegetation. Fig. 8 shows measured air permeability and interpreted lithology. There is a clear relationship between air permeability and lithology. High permeability values, i.e. more than 70,000 mDarcy, are measured in the cross-bedded sands. The lowest permeability values, i.e. lower than 20,000 mDarcy are measured in the clay-rich zones, i.e. the bottomsets and distinct mud drapes. The visual distinction between sand-rich and clay-rich zones that was made in situ is thus relevant for determining different permeability classes.

Figure 9 shows air permeability measurements at a different location made at a smaller spacing. On a 0.6 m by 0.6 m regular grid on a N40°E oriented face, 900 air permeability measurements are made at a spacing of 2 cm. Fig. 9a shows the permeability measurements of this grid plotted on a picture of the quarry wall and Fig. 9b shows the experimental variogram map of measured air permeability which visualizes spatial correlation for different orientations by contouring the variogram. Lamination dip is measured at nine locations in this grid and ranges from 19° to 33° with an average value of 26°. These figures show a relationship between permeability anisotropy and lamination dip. The orientation of strongest

spatial correlation in the experimental variogram corresponds exactly to the dip direction of the laminae. This shows that anisotropy within the cross-bedded sands is determined by foreset lamination.

All 2750 measurements are compiled to obtain histograms and variograms of permeability in the previously defined sand-rich and clay-rich zones. Sand and clay permeability both display a slightly skewed distribution and differ from each other regarding their mean value and spread. Sand permeability displays a higher average permeability and a higher variance. The sand permeability distribution has an average of 58700 mD and a variance of 3.6e8 mD. The clay permeability distribution has an average of 42200 mD and a variance of 2.5e8 (Fig. 10). Sand and clay permeability also display a different spatial structure. The sand variogram is a spherical model with a nugget of 2.09e8 and a sill of 1.51e8. The range in a lamina parallel direction is 0.6 m, the range in a lamina perpendicular direction is 0.3 m. The clay variogram is a spherical model with a nugget of 1.03e8 and a sill of 1.52e8. The range in a lamina parallel direction is 1.9 m, the range in a lamina perpendicular direction is 0.4 m (Fig. 11). Clay permeability thus shows higher anisotropy and larger continuity.

4. Conclusions

In this study, a comparison is made between sedimentary structures and air permeability measurements obtained at a Brussels Sands quarry. The results show that sedimentary heterogeneity induces in permeability heterogeneity. The geometry of the sedimentary structures has a dominant control on permeability. The clay-rich features such as bottomsets and thick mud drapes exhibit a lower permeability than the rest of the cross-bedded sands. This means that these clay-rich layers can act as a flow barrier and compartmentalize the aquifer. Anisotropy in the cross-bedded sands is dominated by the foreset lamination.

Although many geologists in the past have suspected that such a relationship between sedimentary features and permeability should exist in the Brussels Sands, this study is the first to proof and quantify this relation. These results open to the path to much more future research. Now that the permeability heterogeneity due to sedimentary structures is quantified, the effect of this permeability on groundwater flow and transport in the Brussels sands can be investigated. These results can also be extrapolated to the many other aquifers in the world displaying sedimentary structures.

Acknowledgements

The authors wish to acknowledge the Fund for Scientific Research – Flanders for providing a Postdoctoral Fellowship to the first author.

References

Bronders J., 1989, Bijdrage tot de geohydrologie van Midden België door middel van geostatistische analyse en een numeriek model, PhD thesis, Vrije Universiteit Brussel, Brussel

Dykstra H.,and Parsons R.L., 1950, The prediction of oil recovery by waterflood, in Secondary Recovery of Oil in the United States, 2nd edition, Am. Petrol. Inst., Washington, p. 160.

Eijpe R. and Weber K. J., 1971, Mini-permeameters for consolidated rock and unconsolidated sand, AAPG Bulletin, 55, 307-309.

Goggin D. J., Thrasher R. L. and Lake L. W., 1988, A theoretical and experimental analysis of minipermeameter response including gas slippage and high velocity flow effects, In Situ, 12, 79–116.

Halvorsen, C. & Hurst, A. 1990. Principles, practice and applications of laboratory minipermeametry. *In*: Worthington, P. F. (ed.) *Advances in Core Evaluation, Accuracy and Precision in Reserves Estimation.* Gordon & Breach, Amsterdam, 521–549.

Hartkamp C. A., Arribas J., Tortosa A., 1993, Grain-Size, Composition, Porosity and Permeability Contrasts within Cross-Bedded Sandstones in Tertiary Fluvial Deposits, Central Spain, Sedimentology, 40, 4, 787-799.

Houthuys R., 1990, Vergelijkende studie van de afzettingsstruktuur van getijdenzanden uit het Eoceen en van de huidige Vlaamse banken, Aardkundige Mededelingen, Volume 5, Leuven University Press, 137 p.

Hurst, A., and D.J. Goggin. 1995. Probe permeametry: An overview and bibliography. Am. Assoc. Petrol. Geol. Bull. 79:463–473

Jensen J.L., Glasbey C.A. and Corbett P.W.M., 1994, On the Interaction of Geology, Measurement, and Statistical-Analysis of Small-Scale Permeability Measurements, Terra Nova, 6(4), 397-403.

Mikes D., 2006, Sampling procedure for small-scale heterogeneities (crossbedding) for reservoir modelling, Marine and Petroleum Geology, 23, 9-10, 961-977.

Morton K., Thomas S., Corbett P. and Davies D., 2002, Detailed analysis of probe permeameter and vertical inteference test permeability measurements in a heterogeneous reservoir, Petroleum Geoscience, 8, 209-216.

Whittow J.B., 2000, The Penguin Dictionary of Physical Geography, Penguin Books Ltd.

Willis B.J. and White C.D., 2000, Quantitative outcrop data for flow simulation, Journal of Sedimentary Research, v. 70, p. 788-802.

Figure captions

Figure 1 Map of Belgium showing Brussels Sands outcrop and subcrop area (shaded part) and the location of the Bierbeek quarry (modified after Houthuys, 1990)
Figure 2 Sketch of sedimentary structures observed in Brussels Sands: (a) foreset laminae, (b) concave foreset laminae, (c) mud drapes, (d) bottomsets, (e) high-angle reactivation,

(f) convex-upwards reactivation, (g) low-angle reactivations and (h) low-angle foreset lamination (modified after Houthuys, 1990). Height of sketch is approximately 3 m.
Figure 3 Sum of nugget effect model and spherical model
Figure 4 Sketch of bed geometry of Bierbeek quarry faces. Height of sketched walls is approximately 6 m.
Figure 5 Interpreted photomosaic of quarry wall showing clay-rich bottomsets and distinct mud drapes in black. Height of quarry wall is approximately 4 to 5 m.
Figure 6 Histograms of (a) bottomset thicknesses, (b) set thicknesses and (c) lamination dipping angles
Figure 7 Air permeability (mD) projected on a field picture of a 1 m by 1 m 5-cm-spaced regular grid on a N40°E oriented face
Figure 8 Air permeability (mD) projected on a geological sketch of a 1 m by 1 m 5-cm-spaced regular grid on a N40°E oriented face
Figure 9 Air permeability (mD) projected on a field picture of a 0.6 m by 0.6 m 2-cm-spaced regular grid on a N40°E oriented face
Figure 10 Combined histograms of air permeability (mD) of sand-rich and clay-rich zones
Figure 11 Combined variograms of air permeability (mD) of (a) clay-rich and (b) sand-rich zones

Figures

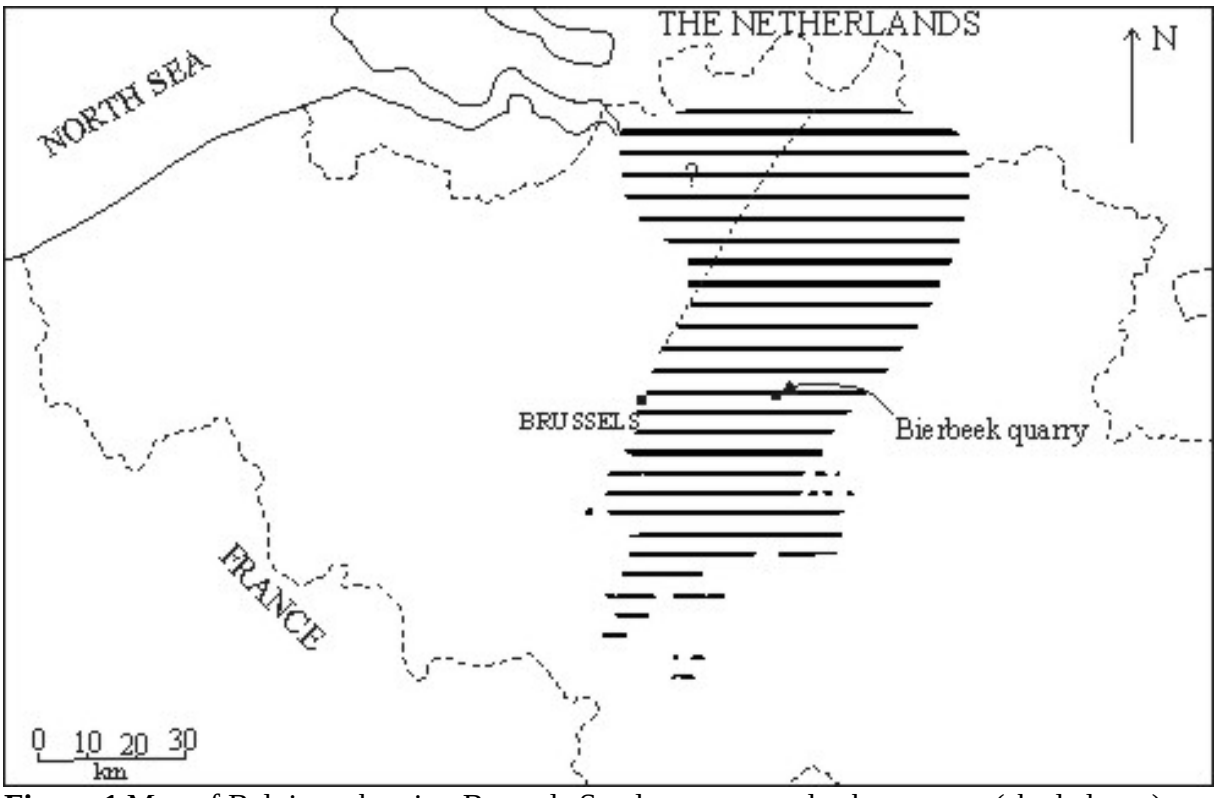

Figure 1 Map of Belgium showing Brussels Sands outcrop and subcrop area (shaded part) and the location of the Bierbeek quarry (modified after Houthuys, 1990)

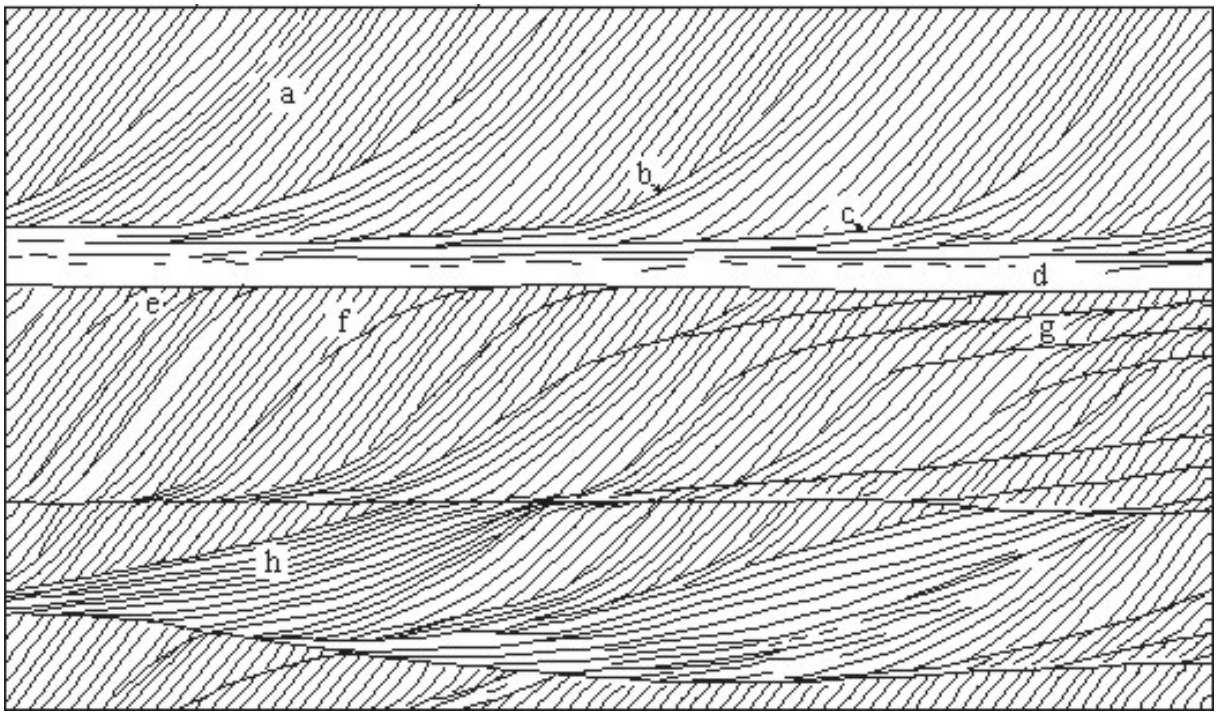

Figure 2 Sketch of sedimentary structures observed in Brussels Sands: (a) foreset laminae, (b) concave foreset laminae, (c) mud drapes, (d) bottomsets, (e) high-angle reactivation, (f) convex-upwards reactivation, (g) low-angle reactivations and (h) low-angle foreset lamination (modified after Houthuys, 1990). Height of sketch is approximately 3 m.

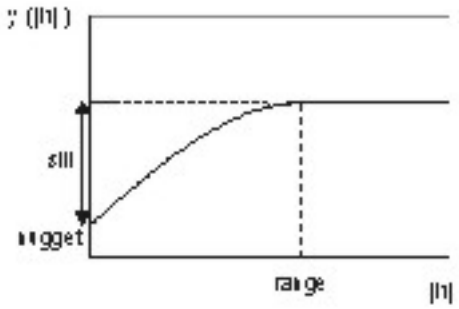

Figure 3 Sum of nugget effect model and spherical model

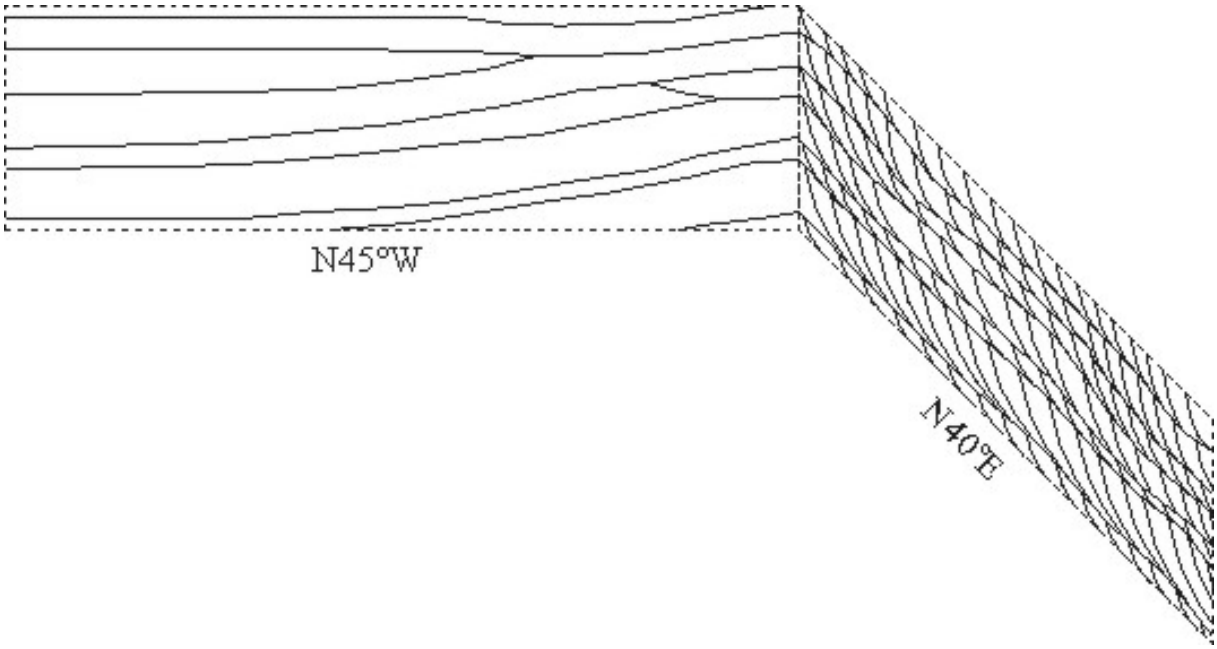

Figure 4 Sketch of bed geometry of Bierbeek quarry faces. Height of sketched walls is approximately 6 m.

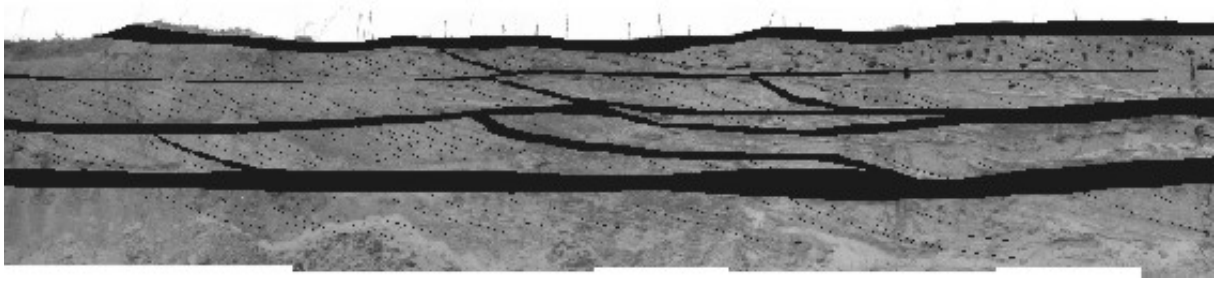

Figure 5 Interpreted photomosaic of quarry wall showing clay-rich bottomsets and distinct mud drapes in black. Height of quarry wall is approximately 4 to 5 m.

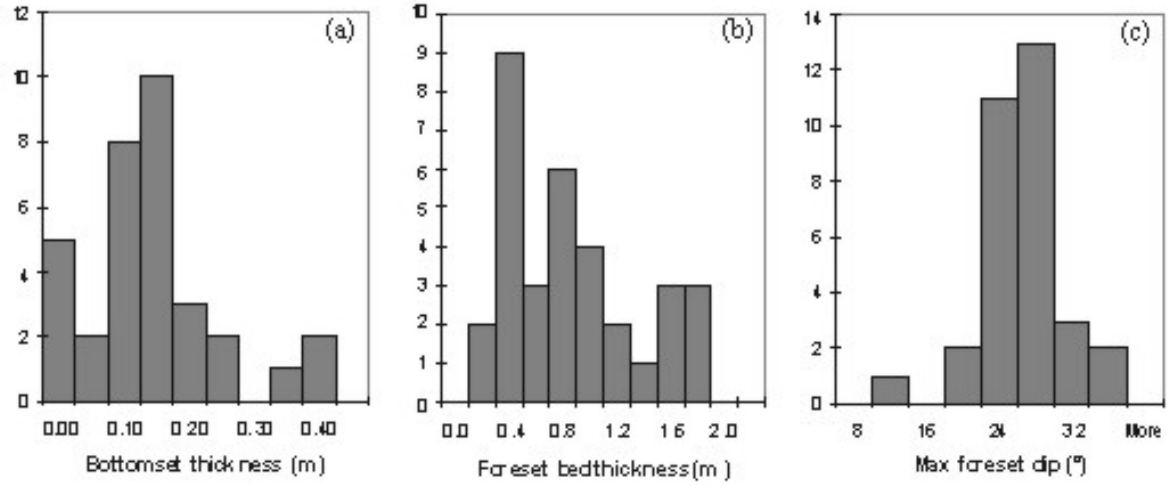

Figure 6 Histograms of (a) bottomset thicknesses, (b) set thicknesses and (c) lamination dipping angles

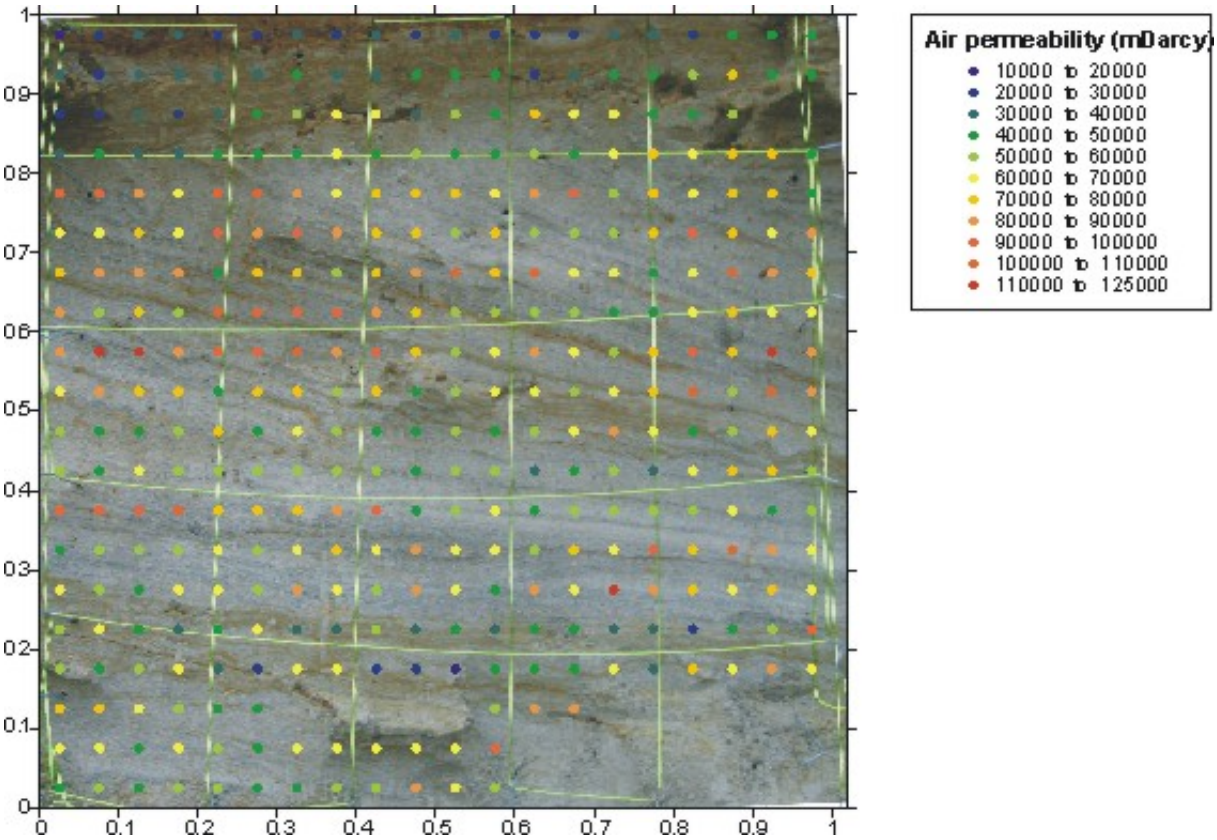

Figure 7 Air permeability (mD) projected on a field picture of a 1 m by 1 m 5-cm-spaced regular grid on a N40°E oriented face

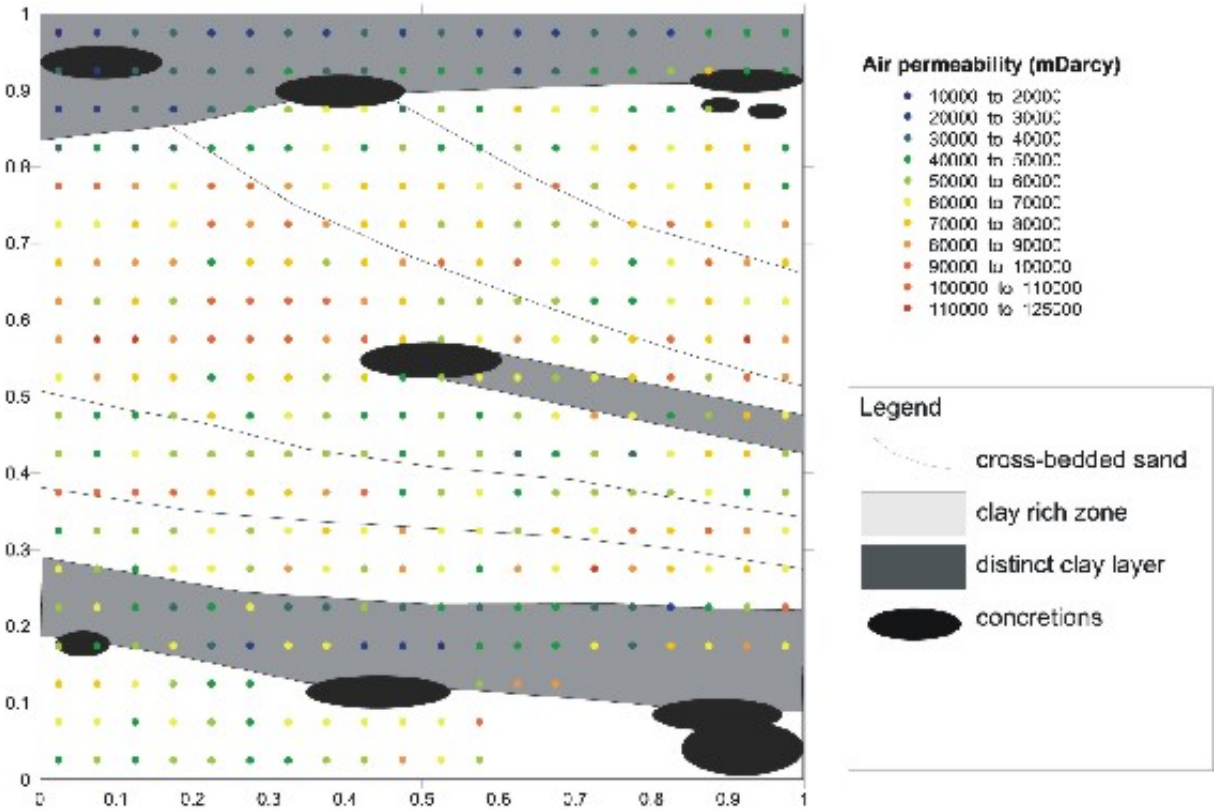

Figure 8 Air permeability (mD) projected on a geological sketch of a 1 m by 1 m 5-cm-spaced regular grid on a N40°E oriented face

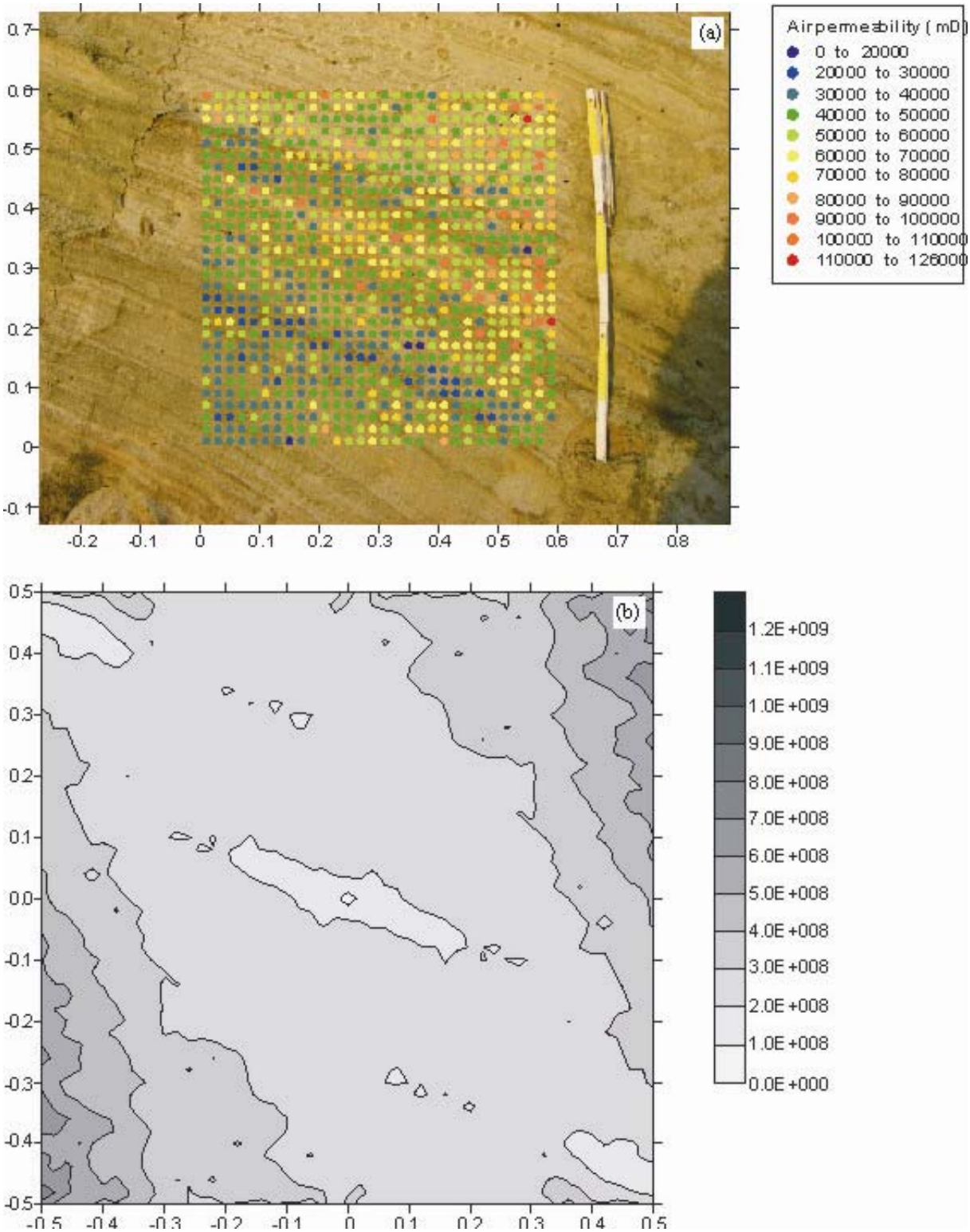

Figure 9 (a) Air permeability (mD) projected on a field picture of a 0.6 m by 0.6 m 2-cm-spaced regular grid on a N40°E oriented face and (b) variogram map of air permeability data

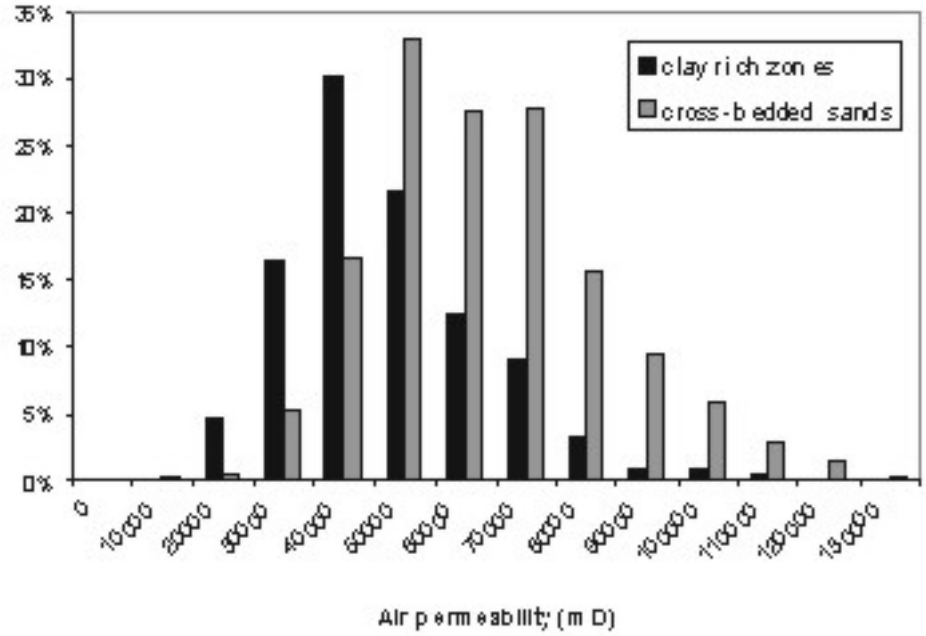

Figure 10 Combined histograms of air permeability (mD) of sand-rich and clay-rich zones

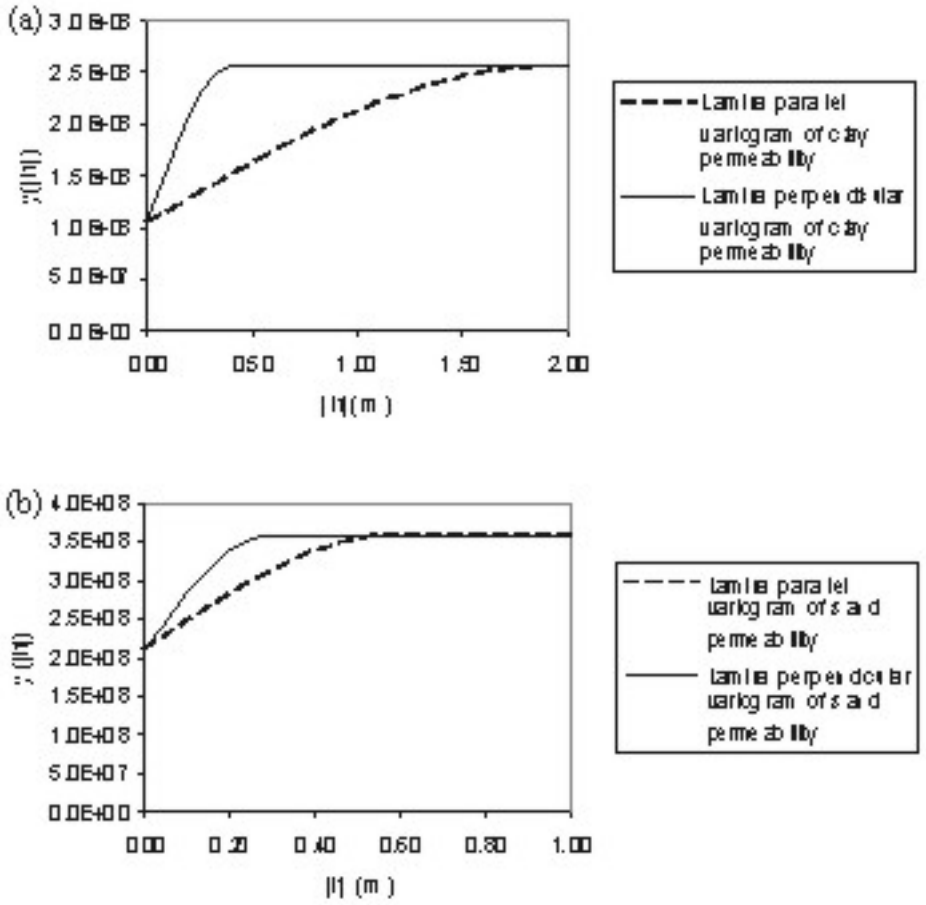

Figure 11 Combined variograms of air permeability (mD) of (a) clay-rich and (b) sand-rich zones